



Microstructural design of 4D printed angle-ply laminated strips with tunable shape memory properties

Yang Liu^a, Fenghua Zhang^b, Jinsong Leng^b, Tsu-Wei Chou^{c,*}

^aState Key Laboratory of New Textile Materials and Advanced Processing Technologies, Wuhan Textile University, Wuhan 430200, PR China

^bCenter for Composite Materials and Structures, Harbin Institute of Technology, Harbin 150080, PR China

^cDepartment of Mechanical Engineering, Center for Composite Materials, University of Delaware, Newark, DE 19716, USA



ARTICLE INFO

Article history:

Received 22 October 2020

Received in revised form 25 November 2020

Accepted 7 December 2020

Available online 11 December 2020

Keywords:

4D printing

Laminates

Polymers

Microstructure

Shape memory property

ABSTRACT

Four-dimensional (4D) printed laminated structures, created by combining three-dimensional (3D) printing technology with shape memory polymer, have tremendous potential for applying in functional devices and sequentially controlled actuators. This work is aimed to study the tunable shape recovery behavior and recovery force of 4D printed laminated strips based on the microstructural design of raster angle and infill percentage. The effects of raster angle and infill percentage on the shape recovery properties of the printed specimens were investigated. The recovery force of the printed specimens was measured using dynamic mechanical analysis (DMA). The microstructural parameters had a significant influence on the shape recovery behavior and recovery force. Finally, the sequential shape-morphing behavior of 4D printed laminated strips using a single material was demonstrated.

© 2020 Published by Elsevier B.V.

1. Introduction

Four-dimensional (4D) printing technology, first introduced in 2013 [1], combines 3D printing methods with stimuli-responsive materials for the development of advanced shape-shifting and function-changing devices. 4D printed devices have been verified tremendous potential in many engineering applications, including robotics [2], origami based actuators [3,4], metamaterials [5] and bioprinting [6]. A range of stimuli-responsive materials for 4D printing has been developed, such as shape memory alloy [7], shape memory polymer (SMP) [8], liquid crystal elastomer [9], composite hydrogel [10], etc. SMP has been extensively used because they can be readily processed and modified.

The development of 4D printed SMP-based devices with tunable shape memory properties has attracted much interest among researchers. For example, Liao et al. [11] developed the tunable multi-stable mechanical metamaterials based on the design of 4D printed SMP unit cells. Qi et al. [12,13] and Teoh et al. [14] reported the tunable shape memory properties for sequential shape-morphing via changing the multi-material composition ratios. They indicate that the multi-stage sequential shape-morphing usually requires multiple materials. However, there are few studies focused on tuning shape memory properties and realizing the

multi-stage sequential shape-morphing using a single material. This work is aimed to study the tunable shape memory properties of the 4D printed single SMP material based on the microstructural design of raster angles and infill percentages. Furthermore, the multi-stage sequential shape-morphing behavior of 4D printed laminated strip using a single material is demonstrated. The specimens were fabricated via the fused deposition modeling (FDM) method. The shape recovery behavior and recovery force of the printed specimens subjected to a bending load were characterized. The microstructural parameters of specimens were investigated in terms of their effects on shape recovery.

2. Materials and methods

2.1. Specimen fabrication

The angle-ply laminated strips were printed by fused deposition modeling (FDM) using polylactic acid (PLA) based SMP filaments. PLA filaments with a diameter of 1.75 mm were prepared by the Harbin Institute of Technology. The glass transition temperature (T_g) of the shape memory PLA was ~ 64 °C [4]. The specimen printing was conducted on a QIDI 3D printer (Qidi Technology Co., China). Based on the findings of our previous work characterizing the filament thermal properties [4], the printer nozzle temperature

* Corresponding author.

E-mail address: chou@udel.edu (T.-W. Chou).

was set at 200 °C and the printing speed at 50 mm/s. The specimen microstructural designs with raster angles of 90°, 90°/0° and ±45° and infill percentages of 33%, 55% and 77% are illustrated in Fig. 1a and b. The angle-ply laminated specimen was composed of 19 layers with mid-plane symmetry. The enlarged optical image of the top view of the 90°/0° printed specimen was given in Fig. S1. All specimens were 60 mm (length) × 12 mm (width) × 5 mm (thickness).

2.2. Characterization of shape recovery behavior and recovery force

During a typical shape memory cycle in this work, the specimen was first heated at 90 °C (higher than T_g) in an oven and deformed into an intermediate L-shape under a bending load. The intermediate L-shape was maintained when the specimen was cooled down to room temperature and unloaded. Upon reheating to 90 °C, the specimen recovered its original shape. The shape recovery evolution was recorded with a Sony video camera. The shape recovery ratio (R_t) of the specimen at recovery time t can be calculated with the following equation: $R_t(\%) = (\theta_t - \theta_i) / (\theta_o - \theta_i) \times 100$. Here, θ_t , θ_i and θ_o denote the bending angles of the specimen shape at the intermediate state, the recovery time t and the original state, respectively. The bending angle θ_t was defined by the specimen top surface, and the measurement method was the same as that in our previous work [15]. The bending angles θ_o and θ_i were around 180° and 90°, respectively.

The characterization of recovery force was as follows. The specimen was uniformly heated at 90 °C in an oven and deformed to an intermediate shape with a curvature radius of 25 mm as subjected to a bending load. The intermediate shape was maintained when it was cooled down to room temperature. The characterization of recovery force of the deformed specimen was conducted using a RSA-G2 DMA (TA Instruments) with bending oscillatory temperature ramp from 25 °C to 90 °C. The temperature ramp rate was 5 °C/min, and a pre-load force of about 0.01 N was applied. The recorded axial force was regarded as the recovery force.

3. Results and discussion

3.1. Shape recovery behavior

Snapshots of the shape recovery process of the 90° printed specimen are shown in Fig. 1c. The specimen starts to recover at 21 s and has almost recovered its original shape at 81 s. Fig. 1d shows the shape recovery ratio vs. time curves of the printed specimens with different raster angles and all at an infill percentage of 33%. These curves show the typical S-shaped recovery, namely a slow recovery rate at the initial and final stages and a fast recovery rate at the middle stage. The average shape recovery rate R_a was defined using the following equation: $R_a(^{\circ}/s) = (\theta_f - \theta_i) / t_f$. Here, θ_f is the final recovery angle, and t_f is the final recovery time. The 90° printed specimen has the largest average recovery rate (1.1°/s) among three printed specimens with different raster angles. The straight and large holes in the 90° printed specimen (Fig. 1b) contribute to faster heat transfer, hence, quicker response. Besides, the 90° printed specimen has a smaller resistance for shape recovery due to its filament orientation being perpendicular to the specimen longitudinal direction (Fig. 1b). The shape recovery ratio vs. time curves of the ±45° printed specimens with different infill percentages are shown in Fig. 1e. The ±45° printed specimen with infill percentage of 77% takes the longest time to recover its original shape; this effect can be attributed to the slow heat conduction rate. The final shape recovery ratios of the printed specimens with infill percentages of 33%, 55% and 77% are 97.5%, 97.1% and 97.6%, respectively. The average shape recovery rates of the ±45° printed specimens decrease in the order of the infill percentages of 33%, 55% and 77%.

3.2. Recovery force

To understand the effect of raster angle and infill percentage on the shape recovery capability, the recovery forces of the 4D printed

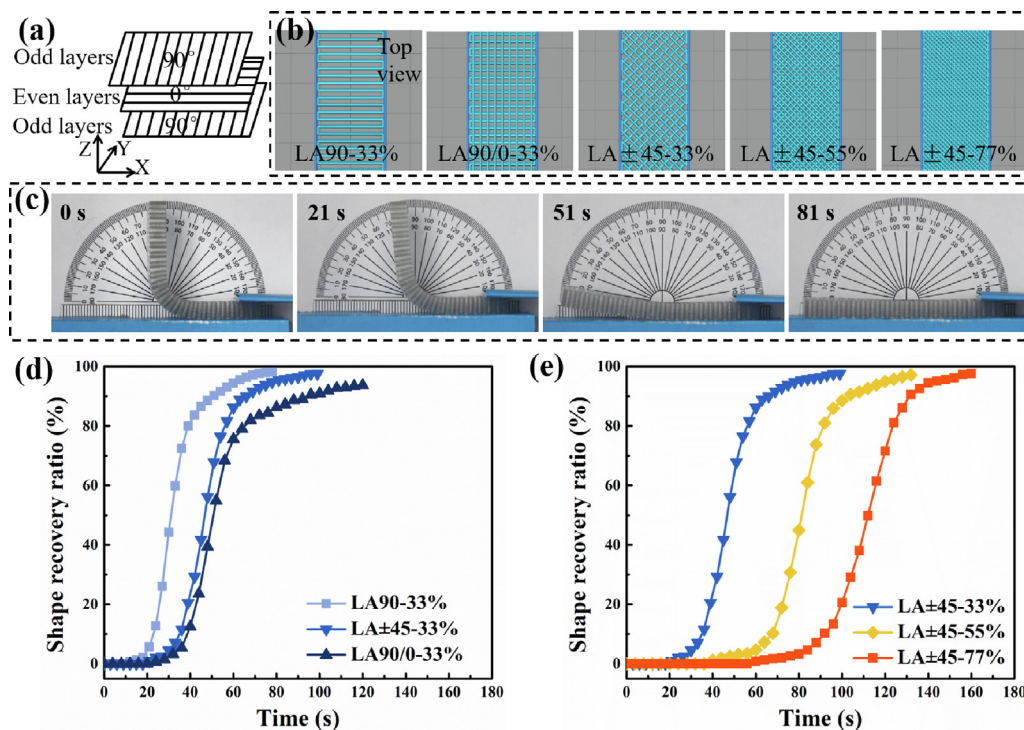


Fig. 1. Microstructural design and shape recovery property of 4D printed laminated specimens. (a) Illustration of raster angles of the 90°/0° printed laminates. (b) Top-viewed models of the printed specimens with different raster angles (90°, 90°/0° and ±45°) and different infill percentages (33%, 55% and 77%). (c) Shape recovery process of the 90° printed specimen at 90 °C. Shape recovery ratio vs. time curves of the printed specimens with (d) different raster angles and (e) different infill percentages.

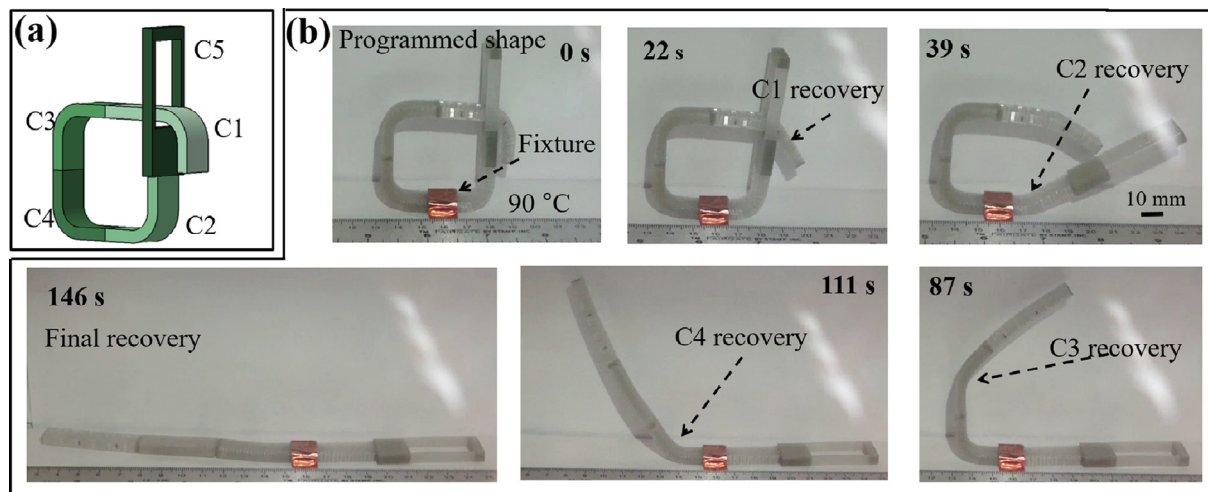


Fig. 3. Demonstration of the sequentially unfolding behavior of 4D printed laminated strip. (a) 3D model of the programmed “locker” with five components. (b) Snapshots of sequentially unfolding behavior of the programmed “locker”.

specimens were characterized and discussed. Fig. 2a shows the recovery force vs. temperature curves of the printed laminates with different raster angles (90°, 90°/0° and ±45°), all at an infill percentage of 33%. As seen in Fig. 2a, when the temperature varies from 25 °C to 43 °C, the recovery force of the ±45° printed specimen first increases to 0.79 N owing to the PLA thermal expansion. Then, up to 57.9 °C, the recovery force of the ±45° printed specimen decreases due to the glass transition zone of PLA. As the temperature increases from 57.9 °C to 90 °C, the recovery force increases due to shape recovery and then decreases owing to temperature-induced softening. The storage modulus rapidly decreases to around 3 MPa during glass transition region and Tan(δ) reaches the peak value at 65 °C (Fig. S2). Due to the contribution of the filament orientation along the longitudinal direction, the recovery force of the printed specimens with raster angles of 90°/0° is larger than that of the specimens of raster angles of 90° and ±45°. Fig. 2b shows the recovery force vs. temperature curves of the ±45° printed specimens with different infill percentages (33%, 55% and 77%). The recovery force of the printed specimen with an infill percentage of 77% shows the largest value among those of the specimens with the three different infill percentages. This can be

attributed to the fact that there are more filaments in the 77% specimens contributing to the recovery force.

3.3. Application

Based on the effect of the microstructural design on shape recovery, the sequentially unfolding behavior can be seen in Fig. 3. A straight active device with five components (C1–C5) was printed. The infill percentages of the components C1, C2, C3, C4 and C5 are 16%, 33%, 55%, 77% and 100%, respectively. The straight active device is first programmed as a “locker”, with the model shown in Fig. 3a. Upon heating at 90 °C, the programmed “locker” can sequentially unfold and recover according to the increasing infill percentages (Fig. 3b).

4. Conclusion

The tunable shape recovery behavior and recovery force of 4D printed laminated strips based on the microstructural design of raster angle and infill percentage were investigated. The raster

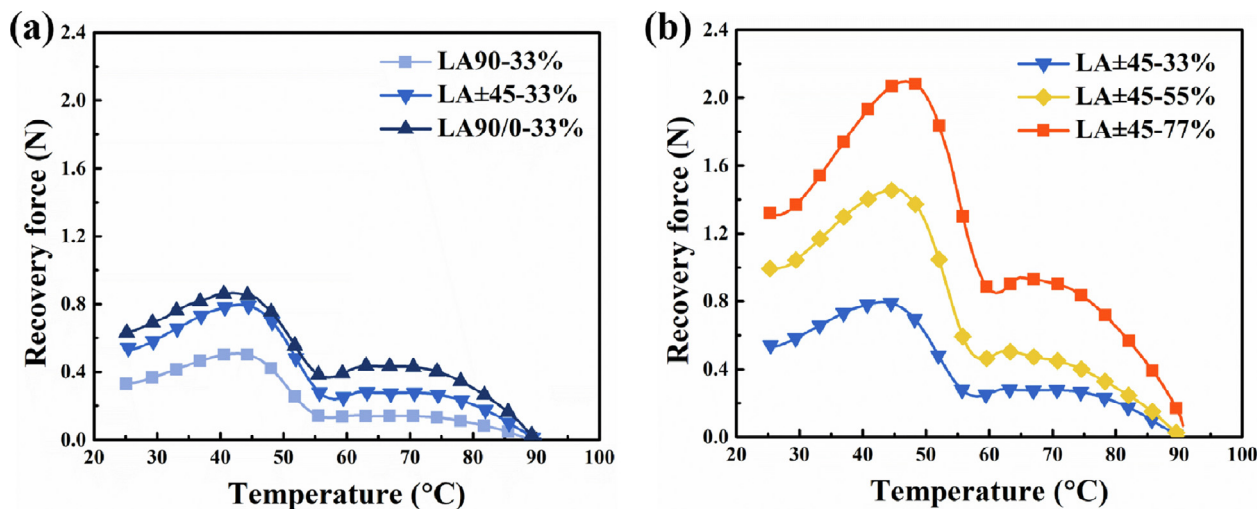


Fig. 2. Recovery force vs. temperature curves of the printed specimens with (a) different raster angles (90°, 90°/0° and ±45°) and (b) different infill percentages (33%, 55% and 77%).

angle has an effect on the shape recovery behavior while its effect is less than that of the infill percentage. The effects of raster angle and infill percentage on the recovery force can be attributed to the filament orientations and material content, respectively. Furthermore, sequential shape-morphing behavior was successfully demonstrated based on various infill percentages of a single SMP.

CRediT authorship contribution statement

Yang Liu: Conceptualization, Methodology, Data curation, Writing - original draft. **Fenghua Zhang:** Resources. **Jinsong Leng:** Resources. **Tsu-Wei Chou:** Writing - review & editing.

Declaration of Competing Interest

The authors declare that they have no known competing financial interests or personal relationships that could have appeared to influence the work reported in this paper.

Acknowledgement

This work was financially supported by the China Scholarship Council.

Appendix A. Supplementary data

Supplementary data to this article can be found online at <https://doi.org/10.1016/j.matlet.2020.129197>.

References

- [1] S. Tibbits, The Emergence of "4D Printing" [TED Talk, 2013.
- [2] S.Y. Hann, H. Cui, M. Nowicki, et al., *Addit. Manuf.* 36 (2020) 101567.
- [3] R. Tao, L. Ji, Y. Li, et al., *Compos. Part B: Eng.* 201 (2020) 108344.
- [4] Y. Liu, W. Zhang, F. Zhang, et al., *Compos. Part B: Eng.* 153 (2018) 233–242.
- [5] M. Bodaghi, A. Damanpack, W. Liao, *Smart Mater. Struct.* 25 (2016) 105034.
- [6] J. An, C.K. Chua, V. Mironov, *Int. J. Bioprint.* 2 (2016) 3–5.
- [7] Z.X. Khoo, Y. Liu, J. An, et al., *Materials* 11 (2018) 519.
- [8] A. Subash, B. Kandasubramanian, *Eur. Polym. J.* 109771 (2020).
- [9] L. Ren, B. Li, Y. He, et al., *ACS Appl. Mater. Interfaces* 12 (2020) 15562–15572.
- [10] M.N.I. Shiblee, K. Ahmed, M. Kawakami, et al., *Adv. Mater. Technol.* 4 (2019) 1900071.
- [11] M. Bodaghi, W. Liao, *Smart Mater. Struct.* 28 (2019) 045019.
- [12] K. Yu, A. Ritchie, Y. Mao, et al., *Proc. Iutam.* 12 (2015) 193–203.
- [13] Y. Mao, K. Yu, M.S. Isakov, et al., *Sci. Rep.* 5 (2015) 13616.
- [14] J. Teoh, J. An, C. Chua, et al., *Virtual Phys. Prototy.* 12 (2017) 61–68.
- [15] Y. Liu, W. Zhang, F. Zhang, et al., *Compos. Sci. Technol.* 107692 (2019).